A Predator-Prey Model with Non-Monotonic Response Function

Broer, H.W.; Naudot, V.; Roussarie, R.; Saleh, K.

Published in:
Regular & chaotic dynamics

DOI:
10.1070/RD2006v011n02ABEH000342

Publication date:
2006

H. W. BROER[1], V. NAUDOT[1], R. ROUSSARIE[2], K. SALEH[1]

[1]**Department of Mathematics, University of Groningen**
P.O. Box 800, 9700 AV Groningen, The Netherlands

[2]**Institut Mathématiques de Bourgogne, CNRS**
9, avenue Alain Savary, B.P. 47 870, 21078 Dijon cedex, France

E-mails: broer@iwi201.iwinet.rug.nl
v.naudot@math.rug.nl
roussari@satie.u-bourgogne.fr
khairul@math.rug.nl

A PREDATOR-PREY MODEL WITH NON-MONOTONIC RESPONSE FUNCTION

Received August 1, 2005; accepted September 1, 2005 DOI: 10.1070/RD2006v011n02ABEH000342

We study the dynamics of a family of planar vector fields that models certain populations of predators and their prey. This model is adapted from the standard Volterra–Lotka system by taking into account group defense, competition between prey and competition between predators. Also we initiate computer-assisted research on time-periodic perturbations, which model seasonal dependence.

We are interested in persistent features. For the planar autonomous model this amounts to structurally stable phase portraits. We focus on the attractors, where it turns out that multi-stability occurs. Further, we study the bifurcations between the various domains of structural stability. It is possible to fix the values of two of the parameters and study the bifurcations in terms of the remaining three. We find several codimension 3 bifurcations that form organizing centers for the global bifurcation set.

Studying the time-periodic system, our main interest is the chaotic dynamics. We plot several numerical examples of strange attractors.

1. Introduction

This paper deals with a particular family of planar vector fields which models the dynamics of the populations of predators and their prey in a given ecosystem. The model is a variation of the Volterra–Lotka system [32], [47] given by

$$\begin{cases} \dot{x} &= x(a-\lambda x) - yP(x), \\ \dot{y} &= -\delta y - \mu y^2 + yQ(x), \end{cases} \tag{1.1}$$

where the variables x and y denote the density of the prey and predator populations respectively, while $P(x)$ is a non-monotonic response function [2] given by

$$P(x) = \frac{mx}{\alpha x^2 + \beta x + 1}. \tag{1.2}$$

Here $\alpha \geqslant 0,\ \delta > 0,\ \lambda > 0,\ \mu \geqslant 0$ and $\beta > -2\sqrt{\alpha}$ are parameters. Observe that in the absence of predators, the prey has logistic growth. The coefficient $a > 0$ represents the intrinsic growth rate of the prey, while λ is the rate of competition or resource limitation of prey. The natural death rate of the predator is given by δ. In Gause's model [25] the function $Q(x)$ is given by $Q(x) = cP(x)$,

Mathematics Subject Classification: 58K45, 34C23, 34C60, 37D45
Key words and phrases: predator-prey dynamics, organizing center, bi-furcation, strange attractor

where $c > 0$ is the rate of conversion between prey and predator. The non-negative coefficient μ is the rate of the competition amongst predators, see [4], [5].

Several experiments by Andrew [2], Boon and Landelout [6] and Edwards [24] indicate that non-monotonic responses are present at the microbial level when the nutrient (prey) concentration reaches a high level, in which case an inhibitory effect on the specific growth rate occurs. Another earlier example of this phenomenon is observed by Tener [45]. Indeed, lone prey (musk ox) can be successfully attacked by predators (wolves). However, small herds of musk oxen (2 to 6 animals) are attacked with less success. Furthermore, no successful attack has been observed in large herds. For more examples of populations that use the group defense strategy, see [40].

Our goal is to understand the structurally stable dynamics of (1.1) and in particular the attractors with their basins where we have a special interest for multi-stability. We also study the bifurcations between the open regions of the parameter space that concern such dynamics, thereby giving a better understanding of the family.

We briefly address the modification of this system, where a small parametric forcing is applied in the parameter λ, as suggested by Rinaldi et al. [38]

$$\lambda = \lambda_0 \left(1 + \varepsilon \sin\left(\frac{2\pi}{\omega} t\right)\right), \tag{1.3}$$

where $\varepsilon < 1$ is a perturbation parameter and ω is a constant. Our main interest is 'large scale' strange attractor.

2. Strategy of research and sketch of results

We now sketch the approach of this paper.

2.1. Trapping domains and Reduced Morse–Smale portraits

Our study concerns the dynamics of (1.1) in the closed first quadrant $\mathrm{clos}(\mathcal{Q})$ where $\mathcal{Q} = \{(x, y) \in \mathbb{R}^2 | x > 0,\ y > 0\}$ with boundary $\partial\mathcal{Q}$, which are both invariant under the flow. We shall show that system (1.1) has a compact *trapping domain* $\mathcal{B}_p \subset \mathrm{clos}(\mathcal{Q})$: all orbits in $\mathrm{clos}(\mathcal{Q})$ enter $\mathcal{B}_p$ after finite time and do not leave it again. For the moment we restrict the attention to structurally stable (or Morse–Smale) dynamics. In the interior of $\mathcal{B}_p$, there can be at most two stable equilibria and possibly one saddle-point. We study these singular points using algebraic tools, occasionally supported by computer algebra. Also we numerically detect several cases with one or two limit cycles. Here we often use numerical continuation, where the algebraic detection of Hopf or Bogdanov–Takens bifurcations helps to initiate the continuation process.

Since limit cycles are hard to detect mathematically, our approach is to reduce, by surgery [33], [35] the structurally stable phase portraits to new portraits without limit cycles. Here with help of topological means (Poincaré–Hopf Index Theorem, Poincaré–Bendixson Theorem [33], [36]) we find a complete classification that is of great help to understand the original system (1.1). Compare with Figure 1 and see Section 3, in particular Theorem 1.

2.2. Organization of the parameter space

As mentioned in Section 1, our main interest is the dense-open subset of the parameter space with structurally stable dynamics. The complement of this set is the bifurcation set, which contains strata of different codimension.

It turns out that the parameters δ and λ play a minor role and that we can describe the bifurcation set as follows. We fix $(\delta, \lambda) \in \Delta$, where $\Delta = \{(\delta, \lambda) \in \mathbb{R}^2 | \delta > 0, \lambda > 0\}$, and the bifurcations of (1.1)

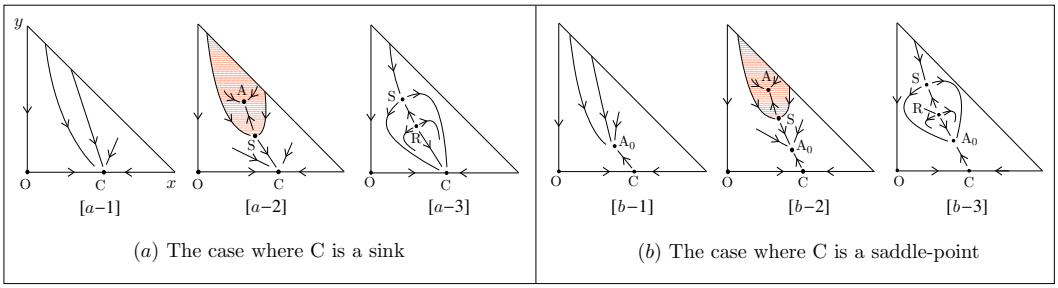

Fig. 1. Reduced Morse–Smale portraits occurring in system (1.1); A is a sink (the corresponding basin is dashed), S is a saddle-point and R a source. (*a*): The case where C is a sink (with corresponding basin in white). (*b*): The case where C is a saddle-point. In the latter case the interior of the trapping domain always contains an attractor denoted by A_0 with basin in white. Bi-stability only occurs in portraits [*a*-2] and [*b*-2].

are described in the space $\mathcal{W} = \left\{(\alpha, \beta, \mu) \in \mathbb{R}^3 | \alpha \geqslant 0, \beta > -2\sqrt{\alpha}, \mu \geqslant 0\right\}$. To discuss this we introduce the projection

$$\Pi : \mathcal{W} \times \Delta \to \Delta,\ (\alpha, \beta, \mu, \delta, \lambda) \mapsto (\delta, \lambda),$$

studying all the fibers $\Pi^{-1}(\delta, \lambda)$. This argument works as long as the fibers are transversal to the bifurcation set consisting of singularities of nilpotent-focus type (NF_3), where we only have to consider bifurcations of codimension less than or equal to 3. It turns out that this is the case in the complement of a smooth curve $\mathcal{C}$, compare with Figure 2*a*. Indeed, as stated in Theorem 2, the bifurcation set in $\mathcal{W}$ is constant above each open region Δ_1 and Δ_2, separated by $\mathcal{C}$. Above the curve $\mathcal{C}$ there is a folding of the bifurcation set whenever the fiber $\Pi^{-1}(\delta, \lambda)$ is tangent to it.

When restricting to Δ_1 and Δ_2 the codimension 3 bifurcations inside $\mathcal{W}$ act as organizing centers. This means that when taking two-dimensional sections in $\mathcal{W}$ we see a semi-global picture organized by the trace of the codimension 3 bifurcations, see [13], [41] for details.

For each region Δ_1 and Δ_2 the associated bifurcation set in $\mathcal{W}$ is depicted in Figure 2*b* and Figure 2*c*, respectively. Figure 2*c* shows that the bifurcation set possesses several codimension 2 curves subordinate to four codimension 3 points which act as organizing centers. Now we explain how to understand the bifurcations up to codimension 1.

2.3. Organizing centers and two-dimensional bifurcation diagrams

Given the organizing centers of the bifurcation sets in $\mathcal{W}$, we take two-dimensional sections $\mathcal{S}_i$, $i = 1, \ldots, 6$, transversal to the codimension 2 curves as indicated in Figure 2. Each two-dimensional section intersects codimension 0 strata in several open regions separated by codimension 1 curves. The two-dimensional bifurcation diagrams are shown, emphasizing the basins of attraction and the possible multi-stability.

We illustrate our strategy in Figure 3 by presenting one of the two-dimensional bifurcation diagrams (in $\mathcal{S}_1$), for the terminology referring to Table 1. For the other two-dimensional diagrams see [13], [41].

2.4. Limit cycles and homoclinic loops

We describe how limit cycles can come into existence by codimension 1 bifurcations. Limit cycles may be created by Hopf bifurcation (H_1) (see for instance regions 1 and 7 of Figure 3), by saddle-node bifurcation of limit cycles ($SNLC_1$) (see regions 9 and 11 of the same Figure 3) and by homoclinic bifurcation (L_1) (or Blue Sky catatrophe [1], see regions 1 and 12 in Figure 3). The occurrence of limit cycles is investigated numerically (continuation) with help of Matlab [28], Matcont [26] and Auto2000 [21].

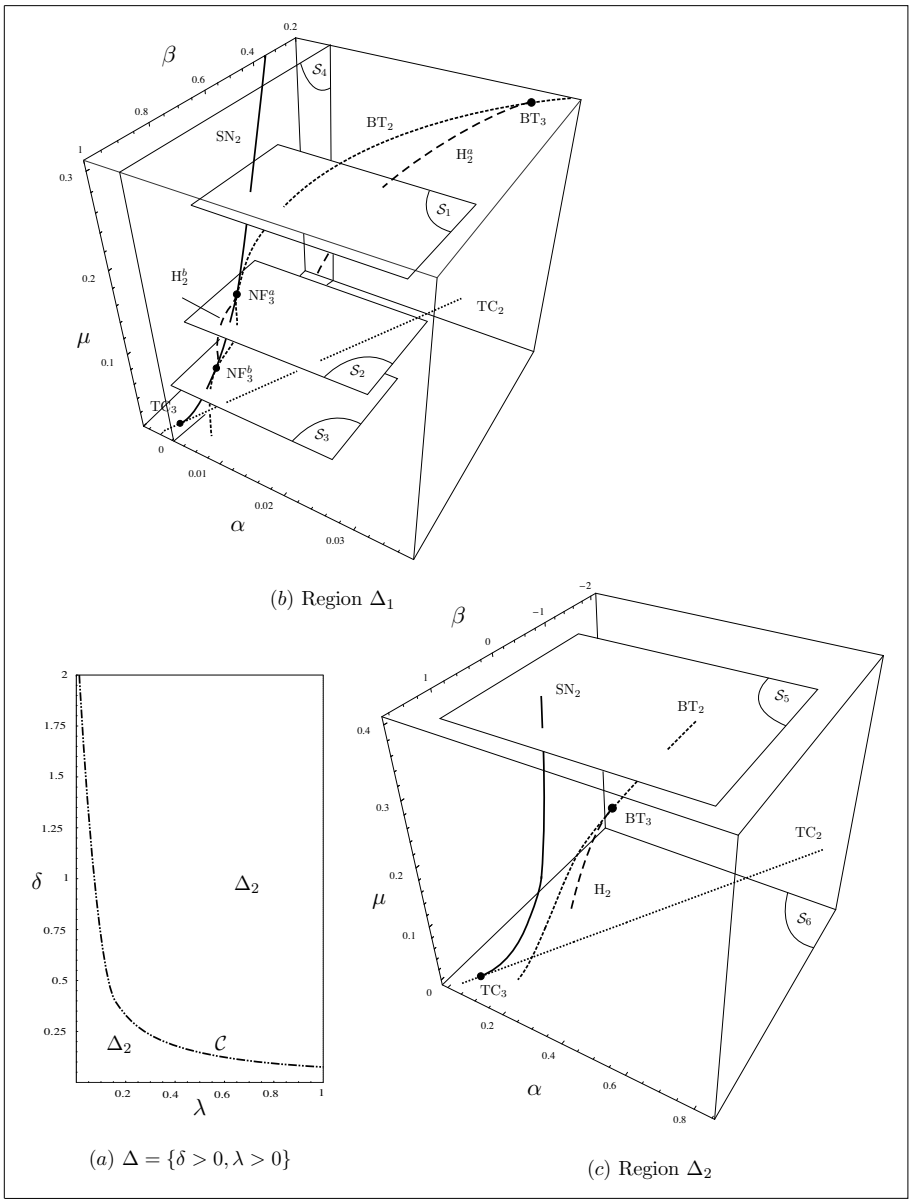

Fig. 2. (a): Region $\Delta = \{\delta > 0, \lambda > 0\}$. ($b$): Bifurcation set in $\mathcal{W} = \{\alpha \geqslant 0, \beta > -2\sqrt{\alpha}, \mu \geqslant 0\}$ when $(\delta, \lambda) \in \Delta_1$. Section $\mathcal{S}_4 = \{\alpha = 0\}$ is the two-dimensional section associated to the bifurcation diagram of Bazykin's model [31]. (c): Similar to (b) for the case $(\delta, \lambda) \in \Delta_2$. Section $\mathcal{S}_6 = \{\mu = 0\}$ covers the case of Zhu's model [50]. For terminology see Table 1.

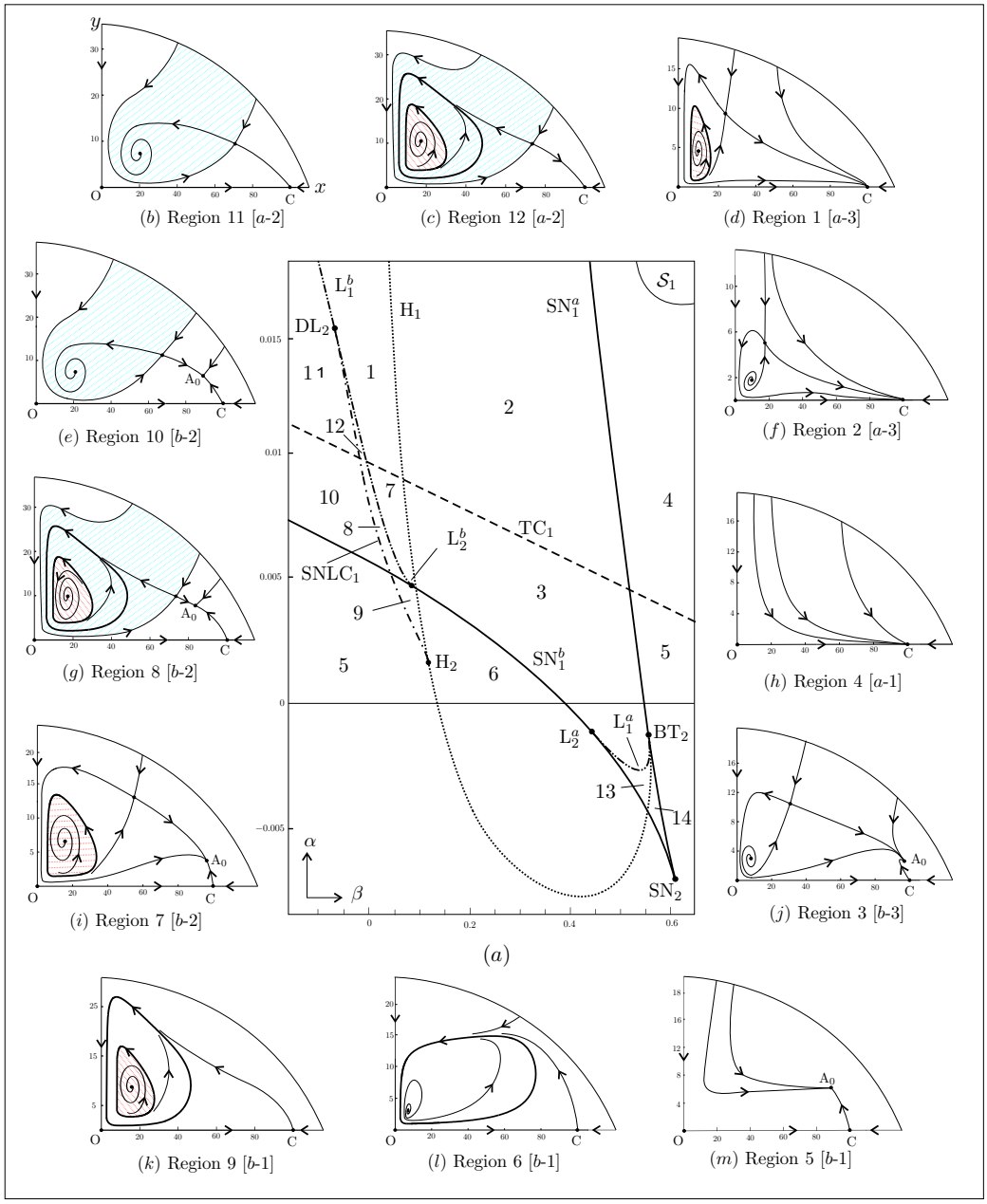

Fig. 3. (a): Bifurcation diagram in two-dimensional section $\mathcal{S}_1 \subset \{\mu = 0.1\}$ of Figure 2-(b), $(\delta, \lambda) = (1.01, 0.01) \in \Delta_1$. A codimension 2 transcritical point lies on the curve TC_1 but is not mentioned since it occurs for $\beta \ll -\sqrt{\alpha}$. Note the presence of a cusp point (SN_2) and a Bogdanov–Takens point (BT_2) below $\{\alpha = 0\}$ both acting as organizing centers. These points are depicted for a better understanding of the bifurcation set. (b)-(n): Associated phase portraits referring to the corresponding Reduced Morse–Smale portraits of Figure 1. Bi-stability in regions 8 and 9 both correspond to [b-2] in Figure 1. Bi-stability also holds in region 7 (corresponding to [b-3], which does not show bi-stability). The basin of attraction in white is either for C or for A_0. For terminology see Table 1.

Notation	Name	Incidence
TC_1	Transcritical	
TC_2	Degenerate transcritical	$SN_1 + TC_1$
TC_3	Doubly degenerate transcritical	$SN_2 + TC_2$
SN_1	Saddle-node	
SN_2	Cusp	$SN_1 + SN_1$
BT_2	Bogdanov–Takens	$SN_1 + H_1 + L_1$
BT_3	Degenerate Bogdanov–Takens	$BT_2 + H_2 + DL_2$
NF_3	Singularity of nilpotent-focus type	$SN_2 + BT_2 + L_2 + H_2$
H_1	Hopf	
H_2	Degenerate Hopf	$H_1 + SNLC_1$
L_1	Homoclinic (or Blue Sky)	
L_2	Homoclinic at saddle-node	$L_1 + SN_1$
DL_2	Degenerate homoclinic	$L_1 + SNLC_1$
$SNLC_1$	Saddle-node of limit cycles	

Table 1. List of bifurcations occurring in system (1.1). This notation will be kept throughout. All bifurcations are local except the latter four, which are global. In all cases the index indicates the codimension of the bifurcation. In the column 'Incidence' we put the subordinate bifurcations of the highest codimension. See [1], [22], [23], [27], [31] for details concerning the terminology and fine structure.

As said before, all local bifurcations can be detected algebraically, which is not the case for the global bifurcations L_1 and $SNLC_1$. Again we resort to numerical continuation methods, using various codimension 2 bifurcations to create initial data. For example, in Figure 3, the degenerate Hopf bifurcation H_2 'generates' the curve $SNLC_1$, while the Bogdanov–Takens bifurcation BT_2 'generates' the curve L_1^a.

2.5. Parametric forcing

Dynamical properties of system (1.1) with parametric forcing (1.3) can be expressed in terms of the stroboscopic map

$$\mathcal{P}_\varepsilon : \mathbb{R}^2 \to \mathbb{R}^2, \quad (x, y) \mapsto \varphi_\varepsilon^1(x, y), \tag{2.1}$$

where φ_ε^t denotes the flow of the time-periodic system written as a three-dimensional vector field $X_\varepsilon = X_\varepsilon(x, y, t; \alpha, \beta, \mu, \delta, \lambda)$.

Fixed points of $\mathcal{P}_\varepsilon$ correspond to periodic solutions of X_ε with period ω, and similarly invariant circles to invariant 2-tori.

We take $|\varepsilon|$ small, so that X_ε is a perturbation of the autonomous system X_0 given in (1.1). As an example, we plot a few attractors for $\mathcal{P}_\varepsilon$ in Figures 4 and 5, for parameter values near the homoclinic curve L_1^b in region 8 of Figure 3. We have numerical evidence for the following statements. Figure 4 shows a strange attractor that consists of 11 connected components mapped by $\mathcal{P}_\varepsilon$ to one another in a cyclic way. These components 'connect' in Figure 5 in a scenario called heteroclinic tangency (or boundary crisis), compare [15].

3. Statement of the results

We formulate the main results of this paper in a more precise way. A brief discussion is included on the behaviour of the stroboscopic map (2.1), based on perturbation theory. The bifurcation sets and the associated phase portraits are drawn with help of Mathematica [49], Matlab [28], Auto2000 [21] and Matcont [26].

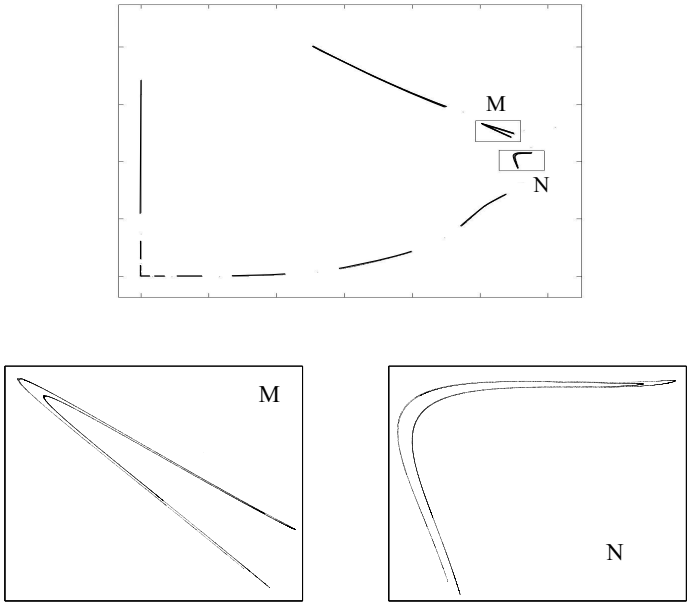

Fig. 4. Top: Strange attractor for $\mathcal{P}_\varepsilon$ for parameter values in region 9 of Figure 3 using 500 000 iterations, $\alpha = 0.007$, $\beta = 0.036$, $\delta = 1.01$, $\mu = 0.1$, $\lambda = 0.01$ and $\varepsilon = 0.6$. The attractor consists of 11 connected components mapped by P_ε to one another in a cyclic way. Left below: Magnification of box M in the figure on the top. Right below: Magnification of box N of the figure on the top.

3.1. Results

The first theorem treats general properties of system (1.1). It contains a classification of the structurally stable case, which covers an dense-open subset of the parameter space $\mathbb{R}^5 = \{\alpha, \beta, \mu, \delta, \lambda\}$. Recall that we only consider the closed first quadrant $\mathrm{clos}(\mathcal{Q})$ of the (x, y)-plane.

Theorem 1. (General properties) *System* (1.1) *has the following properties:*

1. (Trapping domain) *The domain*

$$\mathcal{B}_p = \{(x, y) \mid 0 \leqslant x,\ 0 \leqslant y,\ x + y \leqslant p\}\,,$$

where

$$p > \frac{1}{\lambda}\left(\frac{1}{4\delta}(1-\delta)^2 + 1\right)$$

is a trapping domain, meaning that it is invariant for positive time evolution and also captures all integral curves starting in $\mathrm{clos}(\mathcal{Q})$.

2. (Number of singularities) *There are two singularities on the boundary* $\partial\mathcal{Q}$, *namely* $(0, 0)$ *which is a hyperbolic saddle-point and* $\mathrm{C} = (1/\lambda, 0)$, *which is (semi-) hyperbolic with* $\{(x, y) \in \mathbb{R}^2 | x > 0, y = 0\} \subset W^s(\mathrm{C})$. *In* $\mathcal{Q}$ *there can be no more than three singularities and the cases with zero, one, two and three singularities all occur.*

3. (Classification of the Reduced Morse–Smale case) *Exactly six topological types of Reduced Morse–Smale vector fields occur, listed in Figure* 1.

Sketch of the proof of Theorem 1. Two cases are to be distinguished: either C is a sink or C is a saddle. In the latter case system (1.1) possesses a heteroclinic connection between C and a nearby sink A_0, see Figure 1. Each case leads to three Reduced Morse–Smale portraits. The classification

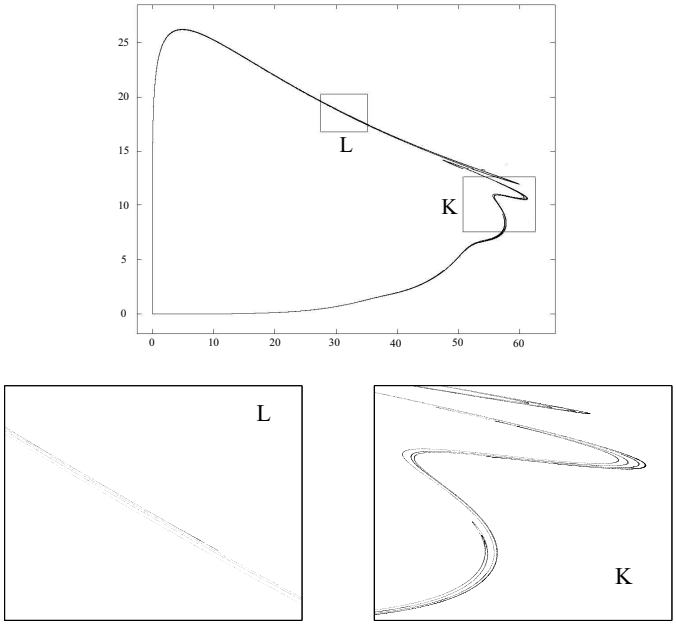

Fig. 5. Top: Viana-like strange attractor for $\mathcal{P}_\varepsilon$ for parameter values in region 9 of Figure 3 using 500 000 iterations, $\alpha = 0.007, \beta = 0.036, \delta = 1.01, \mu = 0.1, \lambda = 0.01$ and $\varepsilon = 0.99$, compare [15]. Left below: Magnification of box L in the figure on the top. Right below: Magnification of box K in the figure on the top.

of the Reduced Morse–Smale phase portraits follows from the Poincaré–Bendixson and the Poincaré–Hopf theorems [33], [36]. To explain this we assume that C is a sink, the case when C is a saddle is treated similarly. For each Reduced Morse–Smale there exists a rectangle $T = PQRS$ included in the trapping domain $\mathcal{B}_p$ with the following properties. The side RS is on the hypothenuse of $\mathcal{B}_p$ and therefore transversal to the flow. The side PQ is situated near C, also transverse to the flow. The sides PS and QR are segments of integral curve of (1.1) and can be chosen arbitrarily close to the coordinates axes such that the rectangle T contains all singularities of (1.1) in $\mathcal{Q}$, see Figure 1. In all cases, the index of the vector field associated to (1.1) with respect to T is equal to 0. This follows from first considering the flow-box case where there are no singularities, see Figure 1 [a-1]. Next we use the fact that the index only depends on the boundary behavior. Knowing that system (1.1) has no more than three singularities in $\mathcal{Q}$, the classification of Figure 1 follows. For details see [13], [41].

The following theorem is illustrated by Figure 2.

Theorem 2. (Organizing centers) *In the parameter space* $\mathbb{R}^5 = \{\alpha, \beta, \mu, \delta, \lambda\}$ *consider the projection* $\Pi : \Delta \times \mathcal{W} \to \Delta$, *where* $\Delta = \{0 < \delta, 0 < \lambda\}$ *and* $\mathcal{W} = \{\alpha \geqslant 0, \beta > -2\sqrt{\alpha}, \mu \geqslant 0\}$. *There exists a smooth curve* $\mathcal{C}$ *that separates* Δ *into two open regions* Δ_1 *and* Δ_2.

For all $(\delta, \lambda) \in \Delta_1$ *the corresponding three-dimensional bifurcation set in* $\mathcal{W}$ *has four organizing centers of codimension* 3 :

1. *One transcritical point* (TC_3),

2. *Two nilpotent-focus type points* (NF_3^a *and* NF_3^b) *connected by a smooth degenerate Hopf curve* (H_2) *and by a smooth cusp curve* (SN_2) *containing* TC_3,

3. *One Bogdanov–Takens point* (BT_3) *connected to* NF_3^b *by a smooth Bogdanov–Takens curve* (BT_2).

Furthermore, the points NF_3^a, NF_3^b *collide when* (δ, λ) *approach* $\mathcal{C}$ *and disappear for* $(\delta, \lambda) \in \Delta_2$. *The organizing centers* TC_3 *and* BT_3 *remain.*

The proof of Theorem 2 is a straight-forward application of classical normal form theory [7], [27], [44] to the system and with help of computer algebra (Mathematica [49]).

REMARK 1. All bifurcations that occur in system (1.1) are known to have finite cyclicity, for definitions and details see [39]. From this it follows that in any compact region of the parameter space, such that the projection under Π is bounded away from the curve $\mathcal{C}$, there is a uniform bound on the number of limit cycles [39]. Although no theoretical information is known on this bound, numerically we find that in our case it is equal to 2.

REMARK 2. From the above remark and Theorem 1 we can give a complete classification of all Morse–Smale types.

3.2. The time-periodic system

As announced in Section 2.5, we here discuss the general relationship between the autonomous system X_0 and the time-periodic perturbation X_ε for $|\varepsilon|$ small.

We consider a number of dynamical properties of $\mathcal{P}_\varepsilon$, as these follow from more or less classical perturbation theory [3], [15], [16], [27]. First of all the hyperbolic periodic points (including fixed points) of $\mathcal{P}_0$ persist for $\mathcal{P}_\varepsilon$, for $\varepsilon \ll 1$, including their local stable and unstable manifolds. We note that globally the stable and unstable manifolds generically will behave different by separatrix splitting, giving rise to homo- and heteroclinic tangle. Secondly, the local bifurcations are persistent, in particular this holds for the saddle-node and cusp of periodic points but also for the Hopf bifurcations of these. In the latter case (for which the three-dimensional vector field X_ε gives Neĭmark–Sacker bifurcations), we encounter resonances due to the interaction of internal periodicity and that of the forcing. The strong resonances are more involved [3], [15], [16], [30], [38], [43], but in the case of weaker resonances, near the Hopf curve, the limit cycle turns into a $\mathcal{P}_\varepsilon$-invariant circle. In a corresponding two-dimensional section in $\mathcal{W}$, the associated rotation number is rational in a dense-open array of Arnol'd tongues emanating from the Hopf curve. Here the circle dynamics is of Kupka–Smale type [36], which corresponds to frequency locking with the periodic forcing. For a large measure set outside the tongues the invariant circles are quasi-periodic with Diophantine rotation number. The invariant circles break up further away from the Hopf curve in a complicated way, compare with [15]. The saddle-node bifurcation of limit cycles in X_0 turns into a quasi-periodic saddle-node bifurcation for $\mathcal{P}_\varepsilon$ [8], [9] with all the ensuing dynamical complexity [17], [18], [19], also compare with [12]. In a systematic study of the attractors of $\mathcal{P}_\varepsilon$ as a function of the parameters, we expect the same complexity as described in [10], [15], [16], [48], for more background also compare with [20], [34], [37]. In this investigation the present study of the autonomous system provides a skeleton.

In this paper we restrict to the numerical detection of a few attractors of $\mathcal{P}_\varepsilon$ near homoclinic connections in the autonomous system X_0.

More precisely we consider the two-dimensional bifurcation diagrams of X_0, looking for the loci of homoclinic orbits (L_1^a and L_1^b in Figure 3). These loci can be continued in the ε-direction for $\varepsilon \geqslant 0$. In particular we look in a neighborhood of L_1^b where complicated dynamics related to homoclinic tangencies are to be expected, compare with Figures 4 and 5. A more systematic approach of this and related time-periodic systems is subject of future research.

4. Summary

We briefly summarize our results. The investigation concerns the dynamics of the predator-prey model (1.1) in the closed first quadrant $\mathrm{clos}(\mathcal{Q})$, where $\mathcal{Q} = \{(x, y) \in \mathbb{R}^2 | x > 0,\ y > 0\}$ with boundary $\partial\mathcal{Q}$ which are both invariant under the flow of (1.1). There are two singularities on the boundary $\partial\mathcal{Q}$: a hyperbolic saddle-point $(0, 0)$ and a (semi-) hyperbolic point $\mathrm{C} = (1/\lambda, 0)$. In $\mathcal{Q}$ there can be no more than three singularities and the cases with zero, one, two and three singularities all occur. The domain has been reduced to a compact *trapping domain* $\mathcal{B}_p \subset \mathrm{clos}(\mathcal{Q})$ which contains all possible singularities, while all orbits in $\mathrm{clos}(\mathcal{Q})$ enter $\mathcal{B}_p$ after finite time and do not leave it

again. Since limit cycles are hard to detect mathematically, our approach is to reduce, by surgery [33], [35], the structurally stable phase portraits to new portraits without limit cycles. With the help of topological means (Poincaré–Hopf Index Theorem, Poincaré–Bendixson Theorem [33], [36]) exactly six topological types of Reduced Morse–Smale Portrait are found; this is of great help to understand the original system (1.1).

To explain the structurally stable dynamics of system (1.1), we investigate bifurcations of the system which separate codimension 0 strata of structurally stable systems. It turns out that in $\Delta = \{(\delta, \lambda) \in \mathbb{R}^2 | \delta > 0, \lambda > 0\}$ there is a curve $\mathcal{C}$ separating Δ into two open regions Δ_1 and Δ_2. In $\mathcal{W} = \{(\alpha, \beta, \mu) \in \mathbb{R}^3 | \alpha \geqslant 0, \beta > -2\sqrt{\alpha}, \mu \geqslant 0\}$ two different bifurcation diagrams are found associated to the two open regions $\Delta_1, \Delta_2 \subset \Delta$. For each region Δ_1 and Δ_2 the corresponding bifurcation set in $\mathcal{W}$ is qualitatively constant and contains several codimension 3 bifurcation points which act as organizing centers of the bifurcation set. We were able to detect all bifurcations of codimension less than or equal to 3, which greatly helps to describe the structurally stable dynamics of (1.1).

We discuss a few biological interpretations of our results regarding model (1.1). Globally speaking there are three possibilities for the coexistence of predators and prey. In the first case the parameters are below the transcritical curve TC_1, compare with Figure 3, which implies that C is a saddle-point. Therefore, independent of the initial values in $\mathcal{Q}$, both prey and predators survive. Compare with regions 3 and 5 in Figure 3. In the second case, only the prey survives, compare with region 4 in Figure 3. In the last case, depending on the initial values in $\mathcal{Q}$, only the prey survives or both prey and predators survive (bi-stability). As an example see region 12 in Figure 3.

Acknowledgement. The authors like to thank Odo Diekmann, Bernd Krauskopf, Kurt Lust, Jean-Christophe Poggiale and Floris Takens for helpful discussions.

References

[1] R. Abraham, J. E. Marsden. *Foundations of Mechanics*. Benjamin Cummings Publishing Company, 1978.

[2] J. F. Andrews. A mathematical model for the continuous of microorganisms utilizing inhibitory substrates. *Biotechnol. Boieng*, **10** (1968), 707–723.

[3] V. I. Arnold. *Mathematical Methods of Classical Mechanics*. GTM V. 60. Springer-Verlag, 1980.

[4] A. D. Bazykin. *Nonlinear dynamics of interacting populations*. World Scientific Series on Nonlinear Science, V. A11. World Scientific, 1998.

[5] A. D. Bazykin, F. S. Berezovskaya, G. Denisov, Yu. A. Kuznetsov. The influence of predator saturation effect and competition among predators on predator-prey system dynamics. *Ecol. Modelling*, **14** (1981), 39–57.

[6] B. Boon, H. Landelout. Kinetics of nitrite oxidation by nitrobacter winogradski. *Biochem. J.*, **85** (1962), 440–447.

[7] H. W. Broer. *Notes on Perturbation Theory 1991*. Erasmus ICP Mathematics and Fundamental Applications. Aristotle University Thessaloniki. 1993.

[8] H. W. Broer, G. B. Huitema, M. B. Sevryuk. *Quasi-Periodic Motions in Families of Dynamical Systems, Order Amidst Chaos*. Lect. Notes in Math. V. 1645. Springer-Verlag. 1996.

[9] H. W. Broer, G. B. Huitema, F. Takens, B. L. J. Braaksma. Unfoldings and bifurcations of quasi-periodic tori. *Mem. AMS*, **83** (1990), №421, 1–175.

[10] H. W. Broer, B. Krauskopf. Chaos in periodically driven systems. In: B. Krauskopf, D. Lenstra (Eds.). *Fundamental Issues of Nonlinear Laser Dynamics*. American Institute of Physics Conference Proceedings, V. 548. 2000, 31–53.

[11] H. W. Broer, R. Roussarie. Exponential confinement of chaos in the bifurcation set of real analytic diffeomorphisms. In: H. W. Broer, B. Krauskopf, G. Vegter (Eds.). *Global Analysis of Dynamical Systems*. Festschrift dedicated to Floris Takens for his 60^{th} birthday. IOP, Bristol and Philadelphia, 2001, 167–210.

[12] H. W. Broer, V. Naudot, R. Roussarie. Catastrophe theory in Dulac unfolding. In: F. Dumortier, H. W. Broer, J. Mawhin, A. Vanderbauwhede, S. M. Verduyn-Lunel (Eds.). Proceedings Equadiff 2003. World Scientific, Singapore, 2003.

[13] H. W. Broer, V. Naudot, R. Roussarie, K. Saleh. Dynamics of a predator-prey model with non-monotonic response function. Preprint, 2005.

[14] H. W. Broer, V. Naudot, R. Roussarie, K. Saleh. Bifurcations of a predator-prey model with non-monotonic response function. *C. R. Acad. Sci. Paris*, Ser. I. **341** (2005), 601-–604.

[15] H. W. Broer, C. Simó, J. C. Tatjer. Towards global models near homoclinic tangencies of dissipative diffeomorphisms. *Nonlinearity*, **11** (1998), 667–770.

[16] H. W. Broer, C. Simó, R. Vitolo. Bifurcations and strange attractors in the Lorenz-84 climate model with seasonal forcing. *Nonlinearity*, **15** (2002), 1205–1267.

[17] A. Chenciner. Bifurcations de points fixes elliptiques. I. Courbes invariantes. *Inst. Hautes Études Sci. Publ. Math.*, **61** (1985), 67–127.

[18] A. Chenciner. Bifurcations de points fixes elliptiques. II. Orbites periodiques et ensembles de Cantor invariants. *Invent. Math.*, **80** (1985), 81–106.

[19] A. Chenciner. Bifurcations de points fixes elliptiques. III. Orbites periodiques de 'petites' périodes et élimination résonnante des couples de courbes invariantes. *Inst. Hautes Études Sci. Publ. Math.*, **66** (1988), 5–91.

[20] L. Díaz, J. Rocha, M. Viana. Strange attractors in saddle cycles: prevalence and globality. *Invent. Math.*, **125** (1996), 37–74.

[21] E. J. Doedel, R. A. Champneys, T. F. Fairgrieve, Yu. A. Kuznetsov, B. Sandstede, X. J. Wang. *AUTO2000: Continuation and Bifurcation Software for Ordinary Differential Equations (with HomCont), User's Guide*. Technical report. Concordia University, Montreal, Canada, 1997-2000. http://indy.cs.concordia.ca

[22] F. Dumortier, R. Roussarie, J. Sotomayor. Generic 3-parameter families of vector fields on the plane, unfolding a singularity with nilpotent linear part. The cusp case of codimension 3. *Ergodic Theory Dynam. Systems*, **7** (1987), 375–413.

[23] F. Dumortier, R. Roussarie, J. Sotomayor, H. Zoladek. *Bifurcations of planar vector fields*. Lect. Notes in Math. V. 1480. Springer-Verlag, 1991.

[24] V. H. Edwards. Influence of high substrate concentrations on microbial kinetics. *Biotechnol. Bioeng.*, **12** (1970), 679–712.

[25] G. F. Gause. Experimental studies on the struggle for existence: I. Mixed population of two species of yeast. *J. Exp. Biol.*, **9** (1932), 389–390.

[26] W. Govaerts, Yu. A. Kuznetsov, A. Dhooge. Numerical continuation of bifurcations of limit cycles in MATLAB. *SIAM J. Sci. Comp.*, **27** (2005), 231—252.

[27] J. Guckenheimer, P. Holmes. *Nonlinear Oscillations, Dynamical Systems, and Bifurcations of Vector Fields*. Springer-Verlag, 1990.

[28] D. Hanselman. *Mastering Matlab*. University of Maine, 2001, http://www.mathworks.com

[29] C. S. Holling. Some characteristics of simple types of predation and parasitism. *Can. Entomolog.*, **91** (1959), 385–398.

[30] B. Krauskopf. Bifurcation sequences at 1:4 resonance: an inventory. *Nonlinearity*, **7** (1994), 1073–1091.

[31] Yu. A. Kuznetsov. *Elements of Applied Bifurcations Theory*. Springer-Verlag, 1995.

[32] A. J. Lotka. *Elements of Physical Biology*. Williams and Wilkins, Baltimore MD, 1925.

[33] J. W. Milnor. *Topology from Differential Viewpoint*. The University Press of Virginia, 1990.

[34] L. Mora, M. Viana. Abundance of strange attractors. *Acta Math.*, **171** (1993), 1-71.

[35] J. R. Munkres. *Elementary Differential Topology*. Princeton Universtity Press, 1963.

[36] J. Palis, W. de Melo. *Geometric Theory of Dynamical System*. Springer-Verlag, 1982.

[37] J. Palis, F. Takens. *Hyperbolicity and sensitive chaotic dynamics at homoclinic bifurcations*. Cambridge Studies in Advanced Mathematics, V. 35. Cambridge University Press, 1993.

[38] S. Rinaldi, S. Muratori, Yu. A. Kuznetsov. Multiple attractors, catastrophes and chaos in seasonally perturbed predator-prey communities. *Bull. Math. Biol.*, **55** (1993), 15–35.

[39] R. Roussarie. *Bifurcations of Planar Vector Fields and Hilbert's Sixteenth Problem*. Progress in Mathematics, V. 164. Birkhäuser, 1998.

[40] S. Ruan, D. Xiao. Global analysis in a predator-prey system with nonmonotonic functional response. *SIAM J. Appl. Math.*, **61** (2001), 1445–1472.

[41] K. Saleh. *Organising centres in the semi-global analysis of dynamical systems*. PhD Thesis. University of Groningen, 2005.

[42] K. Saleh, F. O. O. Wagener. *Semi-global analysis of normal-internal $k:1$ resonances*. Preprint, 2005.

[43] F. Takens. Forced oscillations and bifurcations. In: B. Krauskopf, G. Vegter (Eds.). *Global Analysis of Dynamical Systems*. Festschrift dedicated to Floris Takens for his 60^{th} birthday. IOP, Bristol and Philadelphia, 167–210.

[44] F. Takens. Singularities of vector fields. *Inst. Hautes Études Sci. Publ. Math.*, **43** (1974), 47–100.

[45] J. S. Tener. *Muskoxen*. Queen's Printer, Ottawa, 1965.

[46] R. Thom. *Structural Stability and Morphogenesis*. W. A. Benjamin Inc, 1975.

[47] V. Volterra. Variazioni e fluttuaziono del numero di individui in specie animali conviventi. *Mem. Accad. Lincei.*, **2** (1926), 31–113.

[48] S. Wieczorek, B. Krauskopf, D. Lenstra. A unifying view of bifurcations in a semiconductor laser subject to optical injection. *Optics Communications*, **172** (1999), 279–295.

[49] S. Wolfram. *The Mathematica Book*. Cambridge University Press, Wolfram Research Inc., 1996, http://www.wolfram.com

[50] H. Zhu, S. A. Campbell, G. S. K. Wolkowicz. Bifurcation analysis of a predator-prey system with nonmonotonic functional response. *Siam J. Appl. Math.*, **63** (2002), 636–682.